JOURNAL OF GEOPHYSICAL RESEARCH, VOL. 90, NO. B2, PAGES 1894–1900, FEBRUARY 10, 1985

A Renormalization Group Approach to the Stick-Slip Behavior of Faults

R. F. SMALLEY, JR., AND D. L. TURCOTTE

Department of Geological Sciences, Cornell University, Ithaca, New York

SARA A. SOLLA

Laboratory of Atomic and Solid State Physics
Cornell University, Ithaca, New York

We treat a fault as an array of asperities with a prescribed statistical distribution of strengths. When an asperity fails, the stress on the failed asperity is transferred to one or more adjacent asperities. For a linear array the stress is transferred to a single adjacent asperity and for a two-dimensional array to three adjacent asperities. Using a renormalization group (RG) method, we investigate the properties of a scale invariant hierarchical model for the stochastic growth of fault breaks through induced failure by stress transfer. An extrapolation to arbitrarily large scales shows the existence of a critical applied stress at which the solutions bifurcate. At stresses less than the critical stress, virtually no asperities fail on a large scale, and the fault is locked. Above the critical stress, asperity failure cascades away from the nucleus of failure; we interpret this catastrophic failure as an earthquake and it corresponds to the transition from stick to slip behavior on the fault. Thus the stick-slip behavior of most faults can be attributed to the distribution of asperities on the fault. We propose our stochastic mechanism as an alternative to the traditional hypotheses for the stick-slip behavior of faults. A major advantage of our approach is the inclusion of scale invariance. Thus the observed frequency-magnitude relation for seismicity is a natural consequence of our basic hypothesis.

INTRODUCTION

The worldwide distribution of seismic activity is largely explained by the plate tectonic hypothesis. The relative motion of two surface plates imposes a constant velocity displacement condition on the boundary zone between two plates. This displacement is accommodated by displacements in near-surface fault zones. A fault zone generally includes a number of identifiable faults. A large fraction of the active faults appear to behave in a stick-slip rather than a stable sliding manner. Stress on a fault builds up until a critical condition is reached and a displacement occurs on the fault; this results in an earthquake.

One approach to the understanding of earthquakes is to consider the fracture of a uniform elastic medium subjected to an applied deviatoric stress. Since there is a high density of faults and joints in the earth's crust, it is clearly not appropriate to consider the fracture of pristine rock; however, it may be argued that faults heal, so that a fracture model may be applicable.

An alternative model for the behavior of faults is a planar surface between two elastic half spaces, and the shear resistance to displacement on the boundary is modeled in terms of a coefficient of friction. Several authors have modeled the stick-slip behavior of faults in terms of frictional effects. *Weertmann* [1979] modeled the instability in terms of a frictional stress on a fault that decreases with increasing slip velocity. *Stuart and Mavko* [1979] modeled the instability in terms of a strain-softening constitutive relation for the fault zone.

The direct application of the friction coefficient model to faults predicts that the shear stress τ is given by

$$\tau = f\rho g z \tag{1}$$

where f is the friction coefficient, ρ the crustal density, g the acceleration of gravity, and z the depth. A wide variety of experimental studies on friction predict that the coefficient of friction on a fault should be near 0.8 [*Byerlee*, 1978]. Since earthquakes extend to a depth of 15 km on the San Andreas fault, a model for the stick-slip behavior of a fault must be applicable to this depth. Taking $f = 0.8$, $\rho = 2.8 \times 10^3$ kg m^{-3}, $g = 10$ m s^{-2}, and $z = 15$ km, we find $\tau = 340$ MPa. Any stress associated with fracture and rehealing must be larger than the frictional stress. When applied to the San Andreas fault, the stress level given by the friction hypothesis gives a heat flow anomaly that is much larger than the observed values [*Lachenbruch and Sass*, 1980; *Turcotte et al.*, 1980]. One way to reduce the frictional stress is to require a fluid pressure on the fault that is nearly equal to the lithostatic pressure. However, this is a difficult condition to satisfy in a porous fault zone. Another alternative is to attribute the loss of heat to hydrothermal flows. This alternative has been considered by *Lachenbruch and Sass* [1980] who argue that it is unlikely. Another difficulty of the friction hypothesis is the prediction of a small fractional stress drop during a slip event. Stress drops of about 10 MPa are required by seismic observations and studies of strain fields associated with observed surface offsets on faults. Since the heat flow studies provide evidence that the mean stress on the fault is less than 20 MPa, a significant fractional stress drop is required. The apparent contradiction between the heat flow observations and the laboratory friction measurements is the basis for this paper.

Why might the use of laboratory-derived friction coefficients be an inadequate basis for fault models? We argue that real faults are scale invariant, whereas laboratory friction experiments prescribe a scale. The prescribed laboratory scale is the size of the asperities on the surfaces in contact or the size of the particulate matter placed between the surfaces. An actual fault has asperities and barriers on a wide range of scales. Evidence for scale invariance comes from the wide range of applicability of a power law relationship between earthquake frequency and earthquake magnitude.

Paper number 4B1324.
0148-0227/85/004B-1324$05.00

We compare the behavior of faults to the behavior of the atmosphere and oceans. The laboratory friction experiments may be analogous to laminar flow studies in the laboratory. Laminar flow is not applicable to the atmosphere and oceans because the flow is turbulent. We argue that the behavior of real faults is analogous to the turbulent behavior of the atmosphere and oceans. Over a wide range of scales, turbulence is scale invariant. There are flow eddies with a wide range of sizes in turbulent flow just as there are asperities and barriers with a wide range of sizes on real faults.

An expression of scale invariance is the fractal dimension of a process [*Mandelbrot*, 1982]. The simplest example of scale invariance is the length of the coast line of a rocky island. The length scale l is the length of the rod used to make the measurement. The perimeter P_l (length of the coast line) of the island obtained using a measuring rod of length l is related to the length of the yardstick by

$$P_l \approx l^{1-D} \tag{2}$$

where D is the fractal dimension of the coast line. Note that the length of the coast line increases when measured with a smaller rod because many more small indentations are then included. The fractal dimension of the coast line of Great Britain over a wide range of scales is $D \simeq 1.25$ [*Mandelbrot*, 1967]. Fractal dimensions have been found for a variety of turbulent phenomena. One example is the fractal dimension of the surface of clouds in the atmosphere, with $D \approx 2.35$ [*Hentschel and Procaccia*, 1984]. Turbulent atmospheric processes apparently lead to scale invariance for clouds.

Using frequency-magnitude and moment-magnitude relationships. *Aki* [1981] has shown that the fractal dimension of a fault is $D = 3b/c$, where b is the slope of the log frequency-magnitude relation and c is the slope of the log moment-magnitude relation. For $c = 1.5$ [*Hanks and Kanamori*, 1979] and $b = 1$ the fractal dimension is 2, the same as the topological dimension of a plane [*Aki*, 1981].

Recently, renormalization group (RG) techniques have been successfully applied to scale invariant natural systems [*Wilson and Kogut*, 1974; *Fisher*, 1974]; an example is a system undergoing a continuous phase transition. A characteristic feature of a phase transition is a discontinuous (catastrophic) change of macroscopic parameters of the system under a continuous change in the systems state variables. Clearly, an earthquake is a catastrophic change in the macroscopic response of a fault system.

RG techniques have been used by *Madden* [1983] to relate the macroscopic electrical conductivity and fracture of rocks to the microcrack population and by *Allegre et al.* [1982] to study the coalescence of fractures. *Newman and Knopoff* [1982, 1983] have also studied the coalescence of fractures, and while they use the term renormalization in their work, no rescaling is done, so their approach is substantially different from the usual RG methods.

Formulation of the Problem

In this paper we model a fault as an array of asperities with a statistical distribution of strengths. We will consider both linear and two-dimensional arrays of asperities. In order to illustrate the approach we will first consider a linear array as illustrated in Figure 1. This model should be appropriate for large-scale asperities (barriers) on a long fault. The fault is broken into n elements of length δx, and each element is assigned an asperity failure strength σ_f; the asperity will fail when the stress on the asperity reaches this value. The asperities have a distribution of strengths which will be specified by a statistical distribution function. When a stress σ is applied to the fault, all asperities with a failure strength $\sigma_f < \sigma$ will fail.

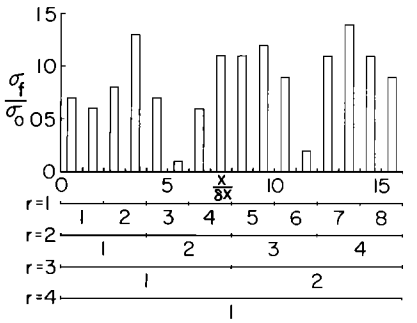

Fig. 1. Illustration of the statistical distribution of asperity strengths σ_f for a linear array; σ_0 is a reference asperity strength. An asperity is assigned to each unit length σx. Also shown are the cell sizes for orders $r = 1$ to 4.

A hierarchical model is now constructed by dividing the linear array of n asperities into $n/2$ cells, each containing two asperities as illustrated in Figure 1. The statistics of cell failure follow from the statistics of asperity failure, since a cell fails only when both asperities in the cell fail. Two alternative processes lead to cell failure. Direct failure results when both asperities break under an applied stress σ. When only one asperity in the cell fails, cell failure may be induced by stress transfer to the unbroken asperity. (The strength σ_f of the unbroken asperity must be greater than 2σ if it is to survive the transfer of stress σ from the broken asperity.) The mechanism for induced failure simulates the transfer of stress to adjacent unbroken regions that occurs when a crack is introduced into an elastic solid. By restricting stress transfer to the interior of a cell we introduce an approximation which renders the problem tractable. A crucial feature included in this approximation is that the size of the unbroken region within which stress is redistributed is of the order of the size of the failed region.

Such a simple mechanism for stress redistribution leads to a complex behavior if used as a basis for a hierarchical model. Subsequent orders in the hierarchy are obtained by treating cells of order r as asperities of order $r + 1$, which are then combined into pairs to obtain cells of order $r + 1$ as illustrated in Figure 1. Confining the redistribution of stress to within cells yields cells that are independent. The use of a hierarchical model introduces a coupling among adjacent cells when they are treated as asperities at the next level of iteration. The hypothesis of scale invariance implies the existence of a unique model description of the system which is independent of length scale except for a prescribed change in the pertinent parameters. Such invariance is the basis for the RG approach. In this case it is implemented through a statistical distribution of asperity strengths which is invariant in that it is the same for asperities of all orders except for an overall renormalization of stress.

The process of stress transfer and induced failure tends to increase the lengths of segments of broken asperities. For a given applied stress the length of the maximum segment of broken asperities is the correlation length. As the applied stress is increased, a value of stress is reached at which the correlation length becomes infinite and failure of an infinite length of asperities occurs. This stress is the critical stress and the value at which the behavior changes catastrophically from stick to slip. The stress at which this change occurs is analo-

gous to the temperature at which a phase transition occurs. The statistical distribution of energies in a solid, liquid, or gas is analogous to the statistical distribution of asperity strengths in our model. The utilization of the RG method allows us to study the development of failed segments as the characteristic lengths of the failed segments increase with increased applied stress.

Our model for fault failure is similar to the one for failure of a fibrous composite material (or a stranded cable). If one strand fails, the stress carried by that strand is transferred to adjacent unbroken strands. Extensive numerical simulations of the failure of composite materials have been carried out [*Harlow and Phoenix*, 1982]. Two results are of interest. The first is that a composite material will fail catastrophically after only a few strands have failed. Second, the load that can be carried is less than the load that can be carried if the strands had been combined into a single, load carrying member. However, an important difference between a fault and a composite material is scale invariance. The scale of a composite material is prescribed by the size of the fibers. Thus an RG approach would not be applicable to its failure.

We next consider the distribution of asperity strengths. Clearly, a wide variety of strengths on a wide variety of scales must exist on any real fault. For example, fault bends and offsets correspond to strong asperities. However, data on actual distributions of asperity strengths are not available. It is possible that studies of the type given in this paper may allow asperity distributions to be inferred from such seismic observations as the dependence of earthquake frequency on magnitude. In the absence of applicable data we assume a quadratic Weibull distribution for the probability P_a that the failure strength σ_f of an asperity is less than the stress $a\sigma$

$$\text{Prob}\ (\sigma_f \leq a\sigma) \equiv P_a = 1 - e^{-(ax)^2} \tag{3}$$

where

$$x = \sigma/\sigma_0$$

and σ_0 is a reference asperity strength. Wiebull distributions are often used to represent a statistical distribution of failure strengths [*Harlow and Phoenix*, 1982]. It should be emphasized that our approach can be applied to any continuous distribution of asperity strengths. The probability

$$P_1 = 1 - e^{-x^2} \tag{4}$$

that $\sigma_f < \sigma$ is shown in Figure 2*a* as a function of σ/σ_0. Ten percent of the asperities have failed when $\sigma/\sigma_0 = 0.32$, fifty percent of the asperities have failed when $\sigma/\sigma_0 = 0.83$, and ninety percent of the asperities have failed when $\sigma/\sigma_0 = 1.52$. Since the relation between P_1 and σ is invertible, P_1 can be used as a measure of the applied stress. The probability density that failure will occur at the applied stress σ/σ_0 is given by dP_1/dx and is shown in Figure 2*b*. The probability density that $\sigma_f = \sigma$ is zero at zero stress and increases to a maximum at $\sigma = 0.71\ \sigma_0$. The mean strength of an asperity is $\bar{\sigma} = (\sqrt{\pi}/2)\sigma_0 = 0.8862\ \sigma_0$.

An essential feature of our model is the transfer of stress from a failed asperity to its nearest neighbors. Without this transfer of stress the behavior of the system is simple and uninteresting. Since strong asperities will not break until large stresses are applied, they can block the propagation of broken segments, and there is no change from stick to slip behavior on the fault. It is the transfer of stress from broken asperities onto the remaining unbroken asperities that leads to catastrophic behavior at an applied stress that is less than the average strength of the asperities. It is clear that stress transfer to the adjacent unbroken sections of a fault will occur on a real fault.

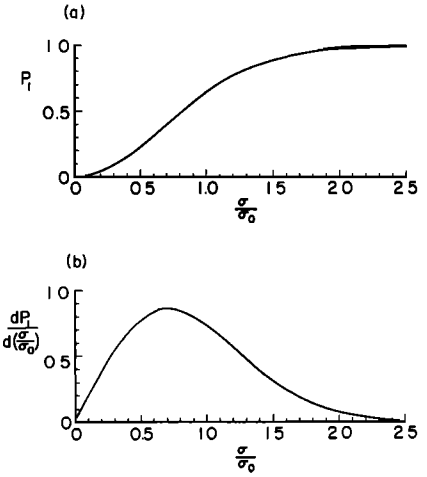

Fig. 2. (*a*) Dependence of the probability P_1 that failure of an asperity will have occurred on the normalized stress σ/σ_0. (*b*) Dependence of the probability that failure will occur at the normalized stress σ/σ_0. This is the change in the probability of failure δP_1 when there is a change in the normalized stress $\delta(\sigma/\sigma_0)$.

In order to quantify the failure of asperities due to the transfer of stress we introduce the conditional probability $P_{a,b}$ that failure will occur when a stress $(a\text{-}b)\sigma$ is transferred to an unbroken asperity supporting a stress $b\sigma$, so that the final stress on the asperity is $a\sigma$. This conditional probability is related to the probability that σ_f is both larger than $b\sigma$ and smaller than $a\sigma$ by [*Meyer*, 1970]

$$P_{a,b} \equiv \frac{\text{Prob}\ (b\sigma < \sigma_f \leq a\sigma)}{\text{Prob}\ (\sigma_f > b\sigma)} \tag{5}$$

A simple geometrical interpretation of both probabilities needed to obtain $P_{a,b}$ follows from the identity

$$P_a = \int_0^{a\sigma/\sigma_0} \frac{dP_1(x)}{dx}\, dx$$

which identifies P_a as the area under the dP_1/dx curve between $x = 0$ and $x = a\sigma/\sigma_0$, shown in Figure 3*a*. Then

$$\text{Prob}\ (b\sigma < \sigma_f \leq a\sigma) = \int_{b\sigma/\sigma_0}^{a\sigma/\sigma_0} \frac{dP_1(x)}{dx}\, dx = P_a - P_b \tag{6}$$

is the area under the $dP1/dx$ curve between $x = b\sigma/\sigma_0$ and $x = a\sigma/\sigma_0$, shown in Figure 3*b*; and

$$\text{Prob}\ (\sigma_f > b\sigma) = 1 - \text{Prob}\ (\sigma_f \leq b\sigma) = 1 - P_b \tag{7}$$

is the area under the dP_1/dx curve between $x = b\sigma/\sigma_0$ and infinity, shown in Figure 3*c*. Substituting (6) and (7) into (5) yields

$$P_{a,b} = \frac{P_a - P_b}{1 - P_b} \tag{8}$$

Note that for a probability function of the form (3),

$$P_a = 1 - (1 - P_1)^{a^2} \tag{9}$$

In principle, this problem could be solved without the use of the RG technique. However, the range of scales that could be studied is quite limited even with the largest computers available. Although we will utilize the RG method in the standard

manner, it should be recognized that the approach is semiempirical and has been principally justified by its success in solving a variety of fundamental unsolved problems in physics. These problems fall in a broad class in which a continuous system on the microscopic scale exhibits discontinuous behavior on the macroscopic scale. We argue that the stick-slip behavior of faults falls in this general classification of physical problems.

We will first illustrate the application of the RG technique to the failure of a linear array of asperities, using a basic cell composed of two "asperities" and the probability distribution given in (2). Note that the $(r+1)$th-order "asperities" which result from r iterations of the RG transformation contain 2^r actual first-order asperities. The first three renormalizations are illustrated in Figure 1. For a cell containing two asperities which are either broken or unbroken, four states are possible: (1) $[bb]$, (2) $[bu]$, (3) $[ub]$, and (4) $[uu]$, where b represents a broken asperity and u represents an unbroken asperity. Note that states 2 and 3 are equivalent and can be combined into a single state with a multiplicity of 2. The probabilities for each of these states, neglecting any interactions between asperities, are given by

$$\begin{array}{ccc} [bb] & [ub] & [uu] \\ P_1^2 & 2P_1(1-P_1) & (1-P_1)^2 \end{array} \tag{10}$$

where the probability of the failure of an individual asperity is P_1.

Next, it is necessary to consider the influence of a broken asperity on an adjacent unbroken asperity. We use the conditional probability $P_{2,1}$ that an unbroken asperity already supporting a stress σ will fail when an additional stress σ is transferred to it from an adjacent broken asperity. This mechanism for transfer of stress leads to induced cell failures. We must prescribe a condition for determining whether an rth order cell is broken or unbroken. We assume that an rth order cell is broken only if both "asperities" in the cell are broken. Probabilities for asperity and cell behavior with stress interactions are

$$\begin{array}{cccc} [bb] & [ub]\rightarrow[bb] & [ub] & [uu] \\ P_1^2 & 2P_1(1-P_1)P_{2,1} & 2P_1(1-P_1)(1-P_{2,1}) & (1-P_1)^2 \\ [bb]+\{[ub]\rightarrow[bb]\} & & [ub]+[uu] & \\ P_1^2+2P_1(1-P_1)P_{2,1} & & (1-P_1)^2+2P_1(1-P_1)(1-P_{2,1}) & \end{array} \tag{11}$$

The conditional probability from (8) is given by

$$P_{2,1}=\frac{P_2-P_1}{1-P_1} \tag{12}$$

Substitution of (12) into (11) gives the probability that a cell has failed $[b_2]$ or not failed $[u_2]$

$$\begin{array}{cc} [b_2] & [u_2] \\ 2P_1P_2-P_1^2 & 1+P_1^2-2P_1P_2 \end{array} \tag{13}$$

Under this condition the probability that a first-order cell is broken, $P_1^{(2)}$, is given by

$$P_1^{(2)}=2P_1P_2-P_1^2 \tag{14}$$

and substitution of P_2 from (9) gives

$$P_1^{(2)}=2P_1[1-(1-P_1)^4]-P_1^2 \tag{15}$$

For higher order cells, (15) is used as an iteration equation to determine $P_1^{(r+1)}$ from $P_1^{(r)}$, where r is the order of the cell being considered. The general form of (15) is

$$P_1^{(r+1)}=2P_1^{(r)}[1-(1-P_1^{(r)})^4]-(P_1^{(r)})^2 \tag{16}$$

Equation (16) implies that a relation of the form (9) between P_1 and P_2 is valid at all orders r, as follows from the assumption of invariance of the statistical distribution of asperity strengths. The probability $P_1^{(r)}$ for failure of an rth-level asperity is given by a Weibull relation of the form (4) in terms of a renormalized stress $\sigma^{(r)}=x^{(r)}\sigma_0$ if

$$(x^{(r+1)})^2=-\ln\{2\exp[-4(x^{(r)})^2]-2\exp[-5(x^{(r)})^2]+\exp[-2(x^{(r)})^2]\} \tag{17}$$

Thus the functional form of the probability distribution is preserved except for an overall stress renormalization, as required by the hypothesis of scale invariance. Our use of a scale invariant model is motivated by evidence of scaling in the nucleation and growth of cracks [*Allegre et al.*, 1982].

The dependence of $P_1^{(r+1)}$ on $P_1^{(r)}$ is given in Figure 4. The points 0 and 1 are stable fixed points of the system. The straight line corresponding to $P_1^{(r+1)}=P_1^{(r)}$ is also included in Figure 4. The iterative relation crosses this straight line at $P_1^{(r)}=P^*=0.2063$. We now show that P^* is an unstable fixed point that separates the region of stick behavior from the region of slip behavior. The RG iteration can be performed graphically using Figure 4. For example, we take $P_1=0.6$ and from (15) find $P_1^{(2)}=0.8093$. This cell behavior at order 1

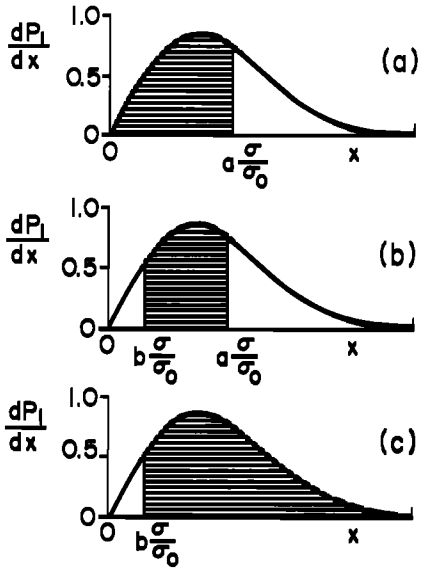

Fig. 3. (*a*) The probability P_a that the failure strength σ_f of a given asperity is less than $a\sigma$ corresponds to the area under the dP_1/dx curve between $x=0$ and $x=a\sigma/\sigma_0$. (*b*) The probability P_a-P_b that the failure strength σ_f of a given asperity lies between $b\sigma$ and $a\sigma$ corresponds to the area under the dP_1/dx curve between $x=b\sigma/\sigma_0$ and $x=a\sigma/\sigma_0$. (*c*) The probability $1-P_b$ that the failure strength σ_f of a given asperity exceeds $b\sigma$ corresponds to the area under the dP_1/dx curve between $x+b\sigma/\sigma_0$ and infinity.

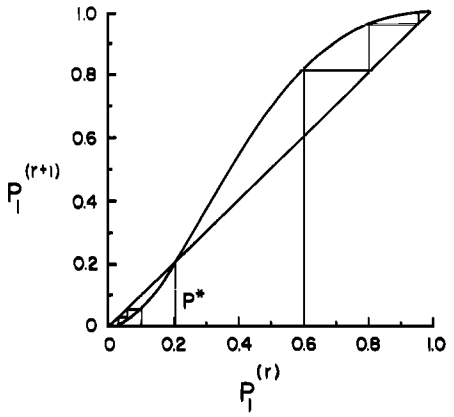

Fig. 4. Dependence of the probability of failure for the $r + 1$ cell $P_1^{(r+1)}$ on the probability of failure of the r cell $P_1^{(r)}$ for cells containing two asperities with a quadratic Weibull distribution of strengths. The procedure described in the text for determining the probability of cell failure for successive iterations is illustrated for $P_1 = 0.6$, 0.1. The critical probability of failure P^* gives the bifurcation point for catastrophic failure of the system. If $P_1 < P^*$, the solution iterates to $P_1^{\infty} = 0$ and no failure occurs. If $P_1 > P^*$, the solution iterates to $P_1^{\infty} = 1$, and the system has failed.

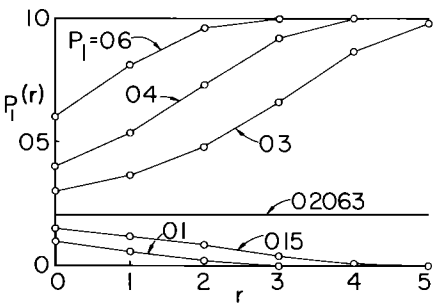

Fig. 5. Dependence of the probability of failure $P_1^{(r)}$ on the order r for several values of P_1. The bifurcation of the solution at $P_1 = P^* = 0.2063$ is clearly illustrated.

now becomes the asperity behavior at order 2. To do this graphically, a horizontal line is extended to the line $P_1^{(r+1)} = P_1^{(r)}$ to reflect the total cell behavior at order 1 into the asperity behavior at order 2. Thus the probability of cell failure at order 2 is $P_1^{(3)} = 0.9615$. This procedure is repeated to give $P_1^{(4)} = 0.9985$, etc., and the probability of failure rapidly approaches unity as the order is increased. On the other hand, if we take $P_1 = 0.1$, we find $P_1^{(2)} = 0.05878$, $P_1^{(3)} = 0.02184$, $P_1^{(4)} = 0.00322$, etc., and the probability of failure decreases towards zero as the order is increased. If $P_1 > P^*$, failure occurs for infinite length scales, and slip behavior results. If $P_1 < P^*$, the behavior is stable, and failure occurs only on the smallest scales. Bifurcation of the solution occurs at $P_1 = P^* = 0.2063$, and the critical stress leading to failure is $\sigma^* = 0.4807\ \sigma_0$ from (3). The corresponding value of $x^* = \sigma^*/\sigma_0 = 0.4807$ is the fixed point solution to the iterative relation (17) for the renormalization of stress. The dependence of $P_1^{(r)}$ on r for several values of P_1 is given in Figure 5. The bifurcation of the solution at $P_1 = P^* = 0.2063$ is clearly illustrated. Note that the value of the critical stress is considerably less than the value of the mean strength of an asperity $\bar{\sigma} = 0.8862\ \sigma_0$.

The stable behavior of the system at $\sigma < \sigma^*$ can be characterized by a correlation length L which measures the maximum length over which failure occurs for $P_1 < P^*$. The rapid increase of L as the threshold is approached from below is described by a power law

$$L \propto (P^* - P_1)^{-\nu} \tag{18a}$$

or equivalently,

$$L \propto (\sigma^* - \sigma)^{-\nu}, \tag{18b}$$

where ν is the correlation length exponent [*Wilson and Kogut*, 1974]. According to this result the magnitude of precursory seismicity would be expected to increase as the critical stress on the fault is approached. The onset of catastrophic behavior at $\sigma = \sigma^*$ corresponds to the divergence of the correlation length L.

The correlation length exponent ν is easily obtained from the RG transformation (16). Given the dependence of $P_1^{(r+1)}$ on $P_1^{(r)}$, the slope of the curve in Figure 4 at $P_1 = P^*$ is given by

$$\Lambda \equiv \left.\frac{dP_1^{(r+1)}}{dP_1^{(r)}}\right|_{P_1 = P^*} \tag{19}$$

As long as $(P^* - P_1^{(r)}) \ll 1$, a linear approximation to (16) is valid, and

$$\Lambda = \frac{P^* - P_1^{(r+1)}}{P^* - P_1^{(r)}} \tag{20}$$

It then follows that [*Wilson and Kogut*, 1974]

$$\Lambda = b^{1/\nu} \tag{21}$$

where b is the linear rescaling factor. For the $b = 2$ RG transformation that led to (16) we obtain $\Lambda = 1.6189$, so that $\nu = 1.4388$.

So far, we have considered only a linear array of asperities. We will next consider a two-dimensional array of asperities distributed uniformly on a planar fault as illustrated in Figure 6. We will divide the two-dimensional array of n asperities into $n/4$ cells each containing four asperities. The failure of individual asperities will be treated in the same way as in the linear case, and (3) is assumed to be applicable. When one or more asperities in a cell fail, we assume that the stress on those asperities is transferred equally to the remaining asperities in the cell. That is, if one asperity fails, the stress on the three remaining asperities is $4\sigma/3$. We choose four asperities in a cell so that the stress in the field region is applied

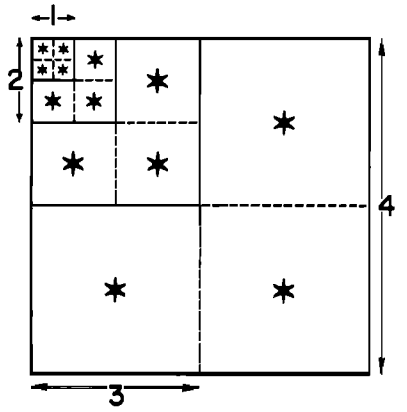

Fig. 6. Illustration of the two-dimensional array of asperities with four asperities per cell. Second (2), third (3), and fourth (4) order cells are also shown.

over a length which is of the order of the length of the failed region. We again assume that the cell fails when all asperities in the cell fail.

A second-order cell is composed of four first-order cells or second-order asperities and therefore sixteen primary asperities, as illustrated in Figure 6. The statistics of failure of the second-order asperities and cells is the same as that of the first-order asperities and cells. Again, the process is repeated by iteration to infinite order. The RG transformation thus constructed corresponds to a linear rescaling factor $b = 2$ on a two-dimensional array. This case is considerably more complex than the linear array example considered above. Following the same procedure illustrated in (10), (11), and (13) and using the definition of the conditional probability, we find that the probability that a cell fails is given by

$$P_1^{(2)} = P_1^{(4)} + 4P_1^3(1 - P_1)P_{4,1} + 6P_1^2(1 - P_1)^2[P_{2,1}^2 + 2P_{2,1}(1 - P_{2,1})P_{4,2}] + 4P_1(1 - P_1)^3\{P_{4/3,1}^3 + 3P_{4/3,1}^2(1 - P_{4/3,1})P_{4,4/3} + 3P_{4/3,1}(1 - P_{4/3,1})^2 \cdot [P_{2,4/3}^2 + 2P_{2,4/3}(1 - P_{2,4/3})P_{4,2}]\} \quad (22)$$

and introducing (8), we obtain

$$P_1^{(2)} = P_1^4 + 4P_1^3(P_4 - P_1) + 6P_1^2(P_2 - P_1)^2 + 12P_1^2(P_2 - P_1)(P_4 - P_2) + 4P_1(P_{4/3} - P_1)^3 + 12P_1(P_{4/3} - P_1)^2(P_4 - P_{4/3}) + 12P_1(P_{4/3} - P_1)(P_2 - P_{4/3})^2 + 24P_1(P_{4/3} - P_1)(P_2 - P_{4/3})(P_4 - P_2) \quad (23)$$

The dependence of $P_1^{(r+1)}$ on $P_1^{(r)}$ shown in Figure 7 follows from introducing P_a from (8) and using (23) as an iterative relation.

The general behavior of this two-dimensional case is the same as that of the linear example considered above. Again, an S-shaped curve is generated. The points 0 and 1 are stable fixed points. The crossing at $P^* = 0.1707$ separates stick from slip behavior. From (3) the bifurcation of the solution occurs at $\sigma^* = 0.4327\ \sigma_0$. This is just about one half the mean strength of the asperities $\sigma = 0.8862\ \sigma_0$. We also find that $\Lambda = 2.357$; the correlation length exponent $\nu = 0.8084$ follows from (20) with $b = 2$. The quantitative differences between

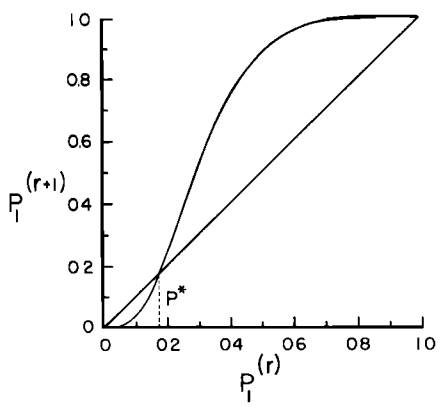

Fig. 7. Dependence of the probability of failure for the $r + 1$ cell $p_1^{(r+1)}$ on the probability of failure of the r cell $P_1(r)$ for cells containing four asperities with a quadratic Weibull distribution of strengths. The critical probability of failure P^* gives the bifurcation point for the system. If $P_1 < P^*$, the solution iterates to $P_1^{\infty} = 0$ and no failure occurs. If $P_1 > P^*$, the solution iterates to $P_1^{\infty} = 1$ and the system has failed.

TABLE 1. Renormalization Group Results for the Critical Probability P^*, the Critical Stress σ^*/σ_0, and the Correlation Length Exponent ν in One and Two Dimensions

d	P^*	σ^*/σ_0	ν
1	0.2063	0.4807	1.4388
2	0.1707	0.4327	0.8084

these results and those for the linear array, as listed in Table 1, illustrate the effect of the physical dimensionality d on the critical behavior of the system. Note the decrease in both the critical probability P^* and the correlation length exponent ν with increasing d. Simpler percolation models exhibit the same trend when d is increased from two to three [*Stauffer*, 1979].

CONCLUSIONS

We have proposed a model for the behavior of faults that is based on the hypothesis of scale invariance. We postulate that fault behavior is controlled by a distribution of asperities and barriers on all scales. In addition to the frictional behavior of fault gouge on the smallest scale, the barriers include bends in the fault and offsets of fault strands. We also lump concentrations of stress and variations of material properties into our statistical approach. We postulate that the asperities and barriers have a statistical distribution of strengths. Scale invariance requires that the same statistical distribution of strengths be applicable at all scales. This is the basis for the applicability of the RG approach. We introduce a mechanism for transfer of stress when an asperity fails. This transfer of stress to adjacent asperities is an essential feature of our approach. However, our results are not qualitatively sensitive to the details of the transfer process, i.e., to how many asperities the stress is transferred to.

The stick-slip behavior of faults is a natural consequence of the renormalization group approach to the statistical model presented here for asperity failure. A critical stress is found at which the catastrophic failure occurs on a macroscopic scale. Below this critical stress, very few precursory fault breaks have occurred. This is in agreement with observations. There is virtually no seismic activity on the locked southern section of the San Andreas fault. We predict that there will be no significant precursory activity on the fault prior to the next great earthquake. We also find that the value of the critical stress is less than the mean strength of the asperities. We believe that this is an explanation for the low stress levels associated with displacements on the San Andreas fault.

Clearly, the model presented in this paper involves many simplifying assumptions and certainly does not predict all aspects of real fault behavior. Some examples are the following:

1. Our analysis predicts that the catastrophic failure extends to infinity. That is, a fault rupture does not terminate. Also, we do not predict the transition from stable sliding to stick-slip behavior. Preliminary studies indicate that both of these difficulties can be overcome by introducing a more complex form for the asperity strength distribution. For instance, a mechanism for blocking the growth of fault breaks can be incorporated into the model by allowing for several peaks rather than a single peak in the probability of failure for a single asperity shown in Figure 2*b*.

2. Our analysis does not predict the fractional stress drop in an earthquake. Obviously, our simple assumption of complete stress transfer to an adjacent asperity neglects any re-

sidual asperity strength and is an oversimplification which can be modified. The failure of a small asperity is equivalent to the introduction of a small dislocation pair on the fault. This will result in a small displacement on the fault whose magnitude is dependent upon the "stiffness" of the adjacent media. When adjacent asperities fail, the size of the dislocation patch grows. This, in turn, allows a larger displacement to occur as long as the failed asperities do not lock.

We would like to emphasize that the approach presented in this paper can be expanded and improved. We consider it to be a preliminary effort to introduce a new approach to the understanding of fault behavior. Our primary purpose is to introduce the concept of scale invariance and some of its implications. Some of the features found in laboratory friction experiments are incorporated through our simple model for asperity behavior, but it is the concept of scale invariance introduced by the RG approach which leads to the results discussed here for the macroscopic behavior of faults.

Acknowledgments. We would like to acknowledge valuable discussions with A. Ruina and F. Horowitz. This research has been supported in part by the National Aeronautics and Space Administration under contract NAS 5-27340 and grant NAG 5-319. This is contribution 766 of the Department of Geological Sciences, Cornell University.

REFERENCES

Aki, K., A probabilistic synthesis of precursory phenomena, in *Earthquake Prediction: An International Review, Maurice Ewing Ser.*, vol. 4, edited by D. W. Simpson and P. G. Richards, pp. 566–574, AGU, Washington, D. C., 1981.

Allegre, C. J., J. L. Le Mouel, and A. Provost, Scaling rules in rock fracture and possible implications for earthquake prediction, *Nature, 297*, 47–49, 1982.

Byerlee, J., Friction of rocks, *Pure Appl. Geophys., 116*, 615–626, 1978.

Fisher, M. E., The renormalization group in the theory of critical behavior, *Rev. Mod. Phys., 46*, 597–616, 1974.

Hanks, T. C., and H. Kanamori, A moment magnitude scale, *J. Geophys. Res., 84*, 2348–2350, 1979.

Harlow, D. G., and S. L. Phoenix, Probability distributions for the strength of fibrous materials under local load sharing, 1, Two-level failure and edge effects, *Adv. Appl. Probab. 14*, 68–94, 1982.

Hentschel, H. G. E., and I. Procaccia, Relative diffusion in tubulent media: The fractal dimension of clouds, *Phys. Rev. A*, in press, 1985.

Lachenbruch, A. H., and J. H. Sass, Heat flow and energetics of the San Andreas fault zone, *J. Geophys. Res., 85*, 6185–6222, 1980.

Madden, T. R., Microcrack connectivity in rocks: A renormalization group approach to the critical phenomena of conduction and failure in crystalline rocks, *J. Geophys. Res., 88*, 585–592, 1983.

Mandelbrot, B., How long is the coast of Britain? Statistical self-similarity and fractional dimension, *Science, 156*, 636–638, 1967.

Mandelbrot, B., *The Fractal Geometry of Nature*, W. H. Freeman, San Francisco, Calif., 1982.

Meyer, P. L., *Introductory Probability and Statistical Applications*, Addison-Wesley, Reading, Mass., 1970.

Newman, W. I., and L. Knopoff, Crack fusion dynamics: A model for large earthquakes, *Geophys. Res. Lett., 9*, 735–738, 1982.

Newman, W. I., and L. Knopoff, A model for repetitive cycles of large earthquakes, *Geophys. Res. Let., 10*, 305–308, 1983.

Stauffer, D., Scaling theory of percolation clusters, *Phys. Rep. 54*, 1–74, 1979.

Stuart, W. D., and G. M. Mavko, Earthquake instability on a strike-slip fault, *J. Geophys. Res., 84*, 2153–2160, 1979.

Turcotte, D. L., P. H. Tag, and R. F. Cooper, A steady state model for the distribution of stress and temperature on the San Andreas fault, *J. Geophys. Res., 85*, 6224–6230, 1980.

Weertman, J., Inherent instability of quasi-static creep slippage on a fault, *J. Geophys. Res., 84*, 2146–2152, 1979.

Wilson, K. G., and J. Kogut, The renormalization group and the ε expansion, *Phys. Rev. C, 12*, 75–200, 1974.

R. F. Smalley, Jr., and D. L. Turcotte, Department of Geological Sciences, Cornell University, Ithaca, NY 14853.

S. A. Solla, Laboratory of Atomic and Solid State Physics, Cornell University, Ithaca, NY 14853.

(Received October 31, 1983;
revised March 27, 1984;
accepted October 26, 1984.)